Molecular Therapy
Original Article

Functional Delivery of Lipid-Conjugated siRNA by Extracellular Vesicles

Aisling J. O'Loughlin,[1] Imre Mäger,[1,2] Olivier G. de Jong,[1] Miguel A. Varela,[1] Raymond M. Schiffelers,[3] Samir El Andaloussi,[1,4] Matthew J.A. Wood,[1] and Pieter Vader[1,3]

[1]Department of Physiology, Anatomy and Genetics, University of Oxford, OX1 3QX Oxford, UK; [2]Institute of Technology, University of Tartu, Tartu 50411, Estonia; [3]Department of Clinical Chemistry and Haematology, University Medical Center Utrecht, 3584 CX Utrecht, the Netherlands; [4]Department of Laboratory Medicine, Clinical Research Center, Karolinska Institutet, SE-141 57 Stockholm, Sweden

Extracellular vesicles (EVs) are cell-derived, membranous nanoparticles that mediate intercellular communication by transferring biomolecules, including proteins and RNA, between cells. As a result of their suggested natural capability to functionally deliver RNA, EVs may be harnessed as therapeutic RNA carriers. One major limitation for their translation to therapeutic use is the lack of an efficient, robust, and scalable method to load EVs with RNA molecules of interest. Here, we evaluated and optimized methods to load EVs with cholesterol-conjugated small interfering RNAs (cc-siRNAs) by systematic evaluation of the influence of key parameters, including incubation time, volume, temperature, and EV:cc-siRNA ratio. EV loading under conditions that resulted in the highest siRNA retention percentage, incubating 15 molecules of cc-siRNA per EV at 37°C for 1 hr in 100 μL, facilitated concentration-dependent silencing of human antigen R (*HuR*), a therapeutic target in cancer, in EV-treated cells. These results may accelerate the development of EV-based therapeutics.

INTRODUCTION

The use of RNA interference (RNAi) to suppress target gene expression is a rational therapeutic strategy for disorders caused by a genetic mutation or by overexpression or aberrant expression of a gene.[1] One hurdle to the successful use of small RNA therapeutics is their delivery. It has been proposed that extracellular vesicles (EVs) may facilitate the delivery of nucleic-acid-based therapeutics across biological barriers, but their use is limited by the difficulty in loading them with cargo of interest.[2] Here, we optimize a method for loading EVs with therapeutic RNA cargo through the use of a lipid-modified anchor on the small interfering RNA (siRNA).

EVs are a heterogeneous population of nanoscale membrane-bound vesicles released from many, if not all, cell types and identified in biological fluids.[3, 4] They consist primarily of exosomes and microvesicles (MVs). Exosomes are of endocytic origin, formed by inward budding of the late endosomal membrane to create intraluminal vesicles (ILVs).[5] These ILVs are released as exosomes upon fusion of the endocytic membrane with the plasma membrane. MVs are secreted by budding or shedding from the plasma membrane.[6]

Increasing evidence suggests that EVs naturally transfer functionally active biomolecules,[7] although studies so far have been mainly limited to demonstrating EV-borne cargo transfer between cells in vitro, and the physiological relevance of such communication remains to be elucidated. Nevertheless, this capacity makes EVs uniquely suited to act as a drug delivery system inspired by nature. They have been used to deliver therapeutic cargo including siRNA in vitro and in vivo, and importantly have been shown to be capable of bypassing biological barriers including the blood-brain barrier (BBB).[8] Despite these advances in the field, clinical development of EVs as therapeutic delivery vehicles is limited by the lack of robust, reproducible, and scalable methods to load them with clinically relevant cargo.

The methods currently used to load EVs include those that capitalize on manipulation of the cell's endogenous RNA sorting machinery and those that are used after EV isolation. Although research is ongoing, the incomplete elucidation of the mechanisms underlying endogenous RNA sorting and resultant lack of efficacy restrict the former approach.[9–11] Transfection has been used for loading following EV isolation, but it is impossible with current technology to completely separate contaminating transfection reagent from loaded EVs.[12–15] Currently, the most commonly used method to load EVs with siRNA is electroporation.[8, 16, 17] Although proof-of-concept studies have shown this method to yield silencing in vivo, several publications have described difficulty in the application of this approach because of a high degree of variability.[16] One explanation for this was described by Kooijmans et al.,[18] who reported that electroporation can induce precipitation and aggregation of the siRNA. This aggregation leads to over-estimation of vesicle loading in the absence of the appropriate controls.

Received 2 December 2016; accepted 13 March 2017;
http://dx.doi.org/10.1016/j.ymthe.2017.03.021.

Correspondence: Matthew J.A. Wood, Department of Physiology, Anatomy and Genetics, University of Oxford, South Parks Road, OX1 3QX Oxford, UK.
E-mail: matthew.wood@dpag.ox.ac.uk
Correspondence: Pieter Vader, Department of Clinical Chemistry and Haematology, University Medical Center Utrecht, Heidelberglaan 100, 3584 CX Utrecht, the Netherlands.
E-mail: pvader@umcutrecht.nl

A

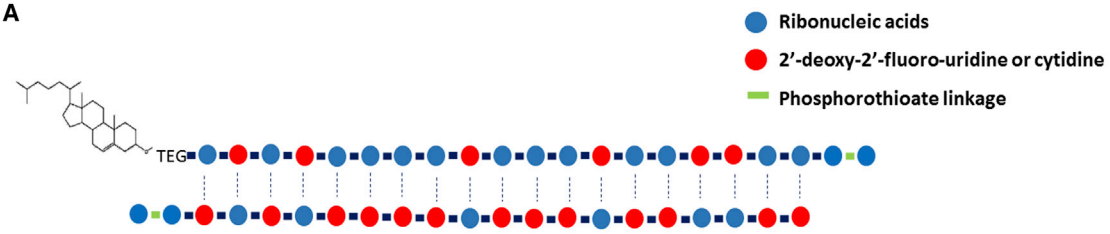

B

	Sense	Antisense
Cy3-HuR siRNA	GUACGGAAUAGAUAAUUAATT	Cy3-UUAAUUAUCUAUUCCGUACTT
Cy3-cc-siRNA HuR	Chol-TEG-GfUAfCGGAAfUAGAfUAAfUfUAA-dTpsdT	Cy3-fUfUAAfUfUAfUfCfUAfUfUfCfCGfUAfC-dTpsdT
cc-siRNA HuR	Chol-TEG-GfUAfCGGAAfUAGAfUAAfUfUAA-dTpsdT	fUfUAAfUfUAfUfCfUAfUfUfCfCGfUAfC-dTpsdT
Control cc-siRNA	Chol-TEG-fUfCGAAGfUAfCfUfCAGfCGfUAAG-dTpsdT	fCfUfUAfCGfCfUGAGfUAfCfUfUfCGA-dTpsdT

C

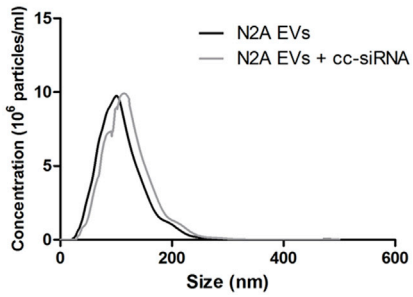

D

	N2A EVs	N2A EVs + cc-siRNA
Mean size (nm) ± SE	110 ± 4	124 ± 5
Mode size (nm) ± SE	99 ± 4	109 ± 4
Total Particles (x10^{10}) ± SE	1.82 ± 0.06	1.83 ± 0.05

E

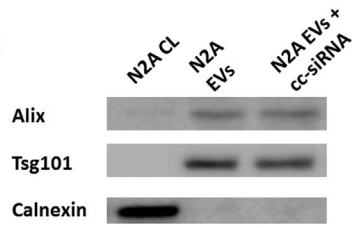

Figure 1. Structure and Sequence of Cholesterol-Conjugated siRNAs and Characterization of EVs after Optimized Incubation with Cholesterol-Conjugated siRNA

(A) Structure of cholesterol-conjugated siRNA (cc-siRNA) showing the 5′ TEG cholesterol, 2′-deoxy-2-fluoro pyrimidines, 19 bp duplex region and phosphorothioate linkages in the 2 bp overhangs. (B) Sequence of human antigen R (*HuR*) siRNAs. Sequences are written in the 5′ to 3′ direction. (C) Size distribution histogram (n = 3) of EVs from Neuro2A cells (N2A EVs) alone or following co-incubation with cc-siRNA and washing (N2A EVs + cc-siRNA), as determined by Nanoparticle tracking analysis (NTA). (D) Table displaying the mean and mode particle size and total number of particles secreted from a 15 cm dish of Neuro2A cells (n = 3) alone (N2A EVs) or following co-incubation with cc-siRNA and washing (N2A EVs + cc-siRNA), as determined by NTA. (E) Western blot probed for the exosomal markers Alix and Tsg101 and the endoplasmic reticulum marker calnexin showing cell lysates (N2A CL), washed EVs (N2A EVs), and washed EVs that had been co-incubated with cc-siRNA (N2A EVs + cc-siRNA). chol, cholesterol; fC 2′-deoxy-2′-fluoro cytidine; fU, 2′-deoxy-2′-fluoro uridine; "ps," phosphorothioate linkage.

Due to the difficulties in loading reported by previous studies, attempts have been made recently to load EVs with hydrophobically modified siRNA.[19, 20] Here, we describe an optimized method to load EVs with cholesterol-conjugated siRNA for functional dose-dependent silencing of the target gene human antigen R (*HuR*), a potential drug target to reduce tumor growth.[21]

RESULTS

Features of Cholesterol-Conjugated siRNA and Characterization of EVs after Co-incubation

The cholesterol-conjugated siRNAs (cc-siRNAs) used in this study comprised a 19 bp duplex region followed by 2 bp phosphorothioated overhangs. Pyrimidines had 2′-deoxy-2-fluoro modifications, and a triethylene glycol (TEG) cholesterol was conjugated to the 5′ sense strand (Figure 1A). The sequences of the *HuR* and control cc-siRNAs are shown in Figure 1B. EVs were isolated from Neuro2A cells using a standard differential ultracentrifugation protocol.[8] Nanoparticle tracking analysis (NTA) showed an EV size distribution from 50 to 250 nm, peaking at 100 nm (Figures 1C and 1D). Western blotting analysis confirmed that EV marker proteins Alix and Tsg101 were enriched in EVs compared with cell lysate, whereas the opposite was observed for the endoplasmic reticulum protein calnexin (Figure 1E).

Optimization of Loading via Co-incubation

Given the lipophilic nature of cholesterol, we hypothesized that cc-siRNA would self-associate with EVs after simple co-incubation. Therefore, various parameters of co-incubating cc-siRNA with EVs were investigated to establish the optimal conditions for maximum association, including temperature, incubation time, and volume, and the ratio of cc-siRNA to EVs.

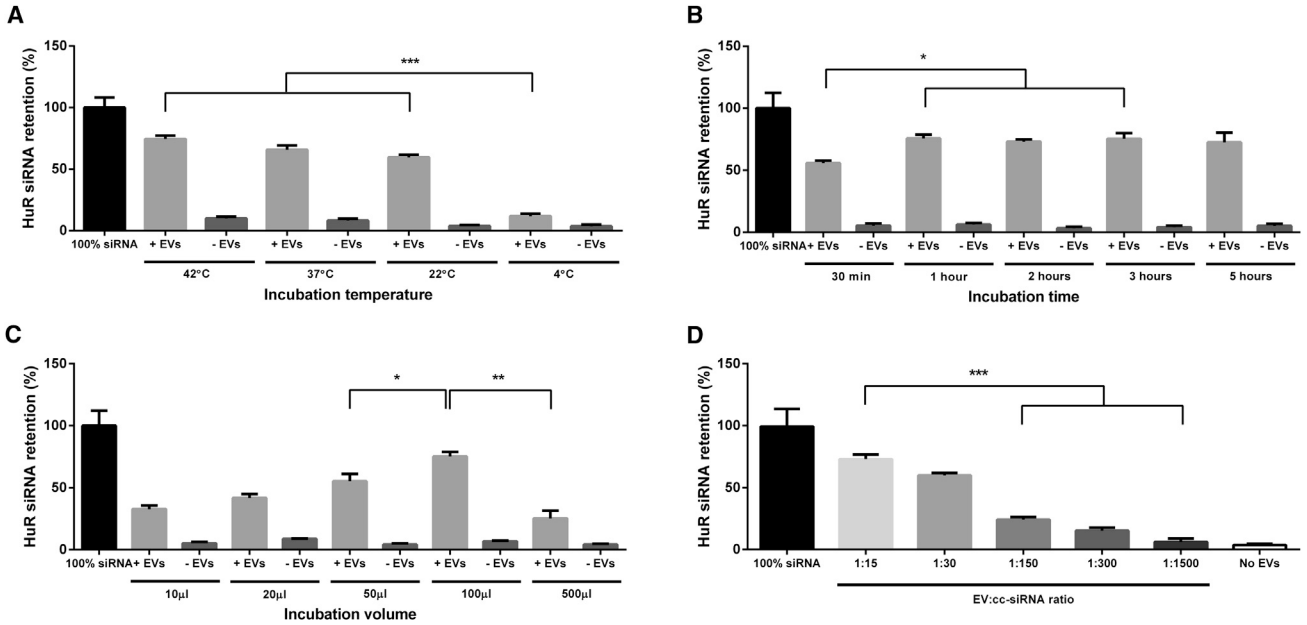

Figure 2. Optimization of Conditions for Loading of EVs with cc-siRNA

EVs derived from Neuro2A cells were mixed with fluorescent cc-siRNA to optimize the conditions of loading via co-incubation. Samples were concentrated and washed by ultracentrifugation, the pellet resuspended in PBS, and the resultant quantity of cc-siRNA in the pellet was assessed by plotting the signal of samples containing EVs (+EVs) and without EVs (−EVs) against that of a standard curve of the original quantity of input cc-siRNA (100% siRNA) as measured by fluorescence. (A) siRNA retention in pellet following mixing of EVs with cc-siRNA with varying incubation temperature. EVs were mixed with fluorescent cc-siRNA at a ratio of 1:30 at various incubation temperatures for 30 min in 100 µL PBS. (B) siRNA retention in pellet following mixing of EVs with cc-siRNA with varying incubation time. EVs were mixed with fluorescent cc-siRNA at a ratio of 1:30 at incubation temperatures of 37°C in 100 µL. (C) siRNA retention in pellet following mixing of EVs with cc-siRNA with varying incubation volume. EVs were mixed with fluorescent cc-siRNA at a ratio of 1:30 at incubation temperatures of 37°C for 1 hr in various volumes of PBS. (D) siRNA retention in pellet following mixing of EVs with cc-siRNA with varying EV:cc-siRNA ratios. Samples were incubated at room temperature for 30 min in 100 µL. Values represent mean + SEM, n = 3. Statistical differences were calculated by one-way ANOVA followed by Tukey's post hoc analysis. ***$p < 0.001$, **$p < 0.01$, *$p < 0.05$.

First, to assess the effect of incubation temperature on EV loading by co-incubation, we mixed EVs with a fixed amount (20 pmol) of cc-siRNA at a ratio of 30 molecules of cc-siRNA per EV in 100 µL for 30 min at varying temperatures. This was performed both in the presence and the absence of EVs to control for the possibility that increasing temperature may increase the likelihood of cc-siRNA precipitating with the EVs in the pellet (Figure 2A).

Mixing at 4°C resulted in a low level (12%) of cc-siRNA retention in the pellet indicating low levels of incorporation of cc-siRNA into the vesicles. This was expected because at 4°C the EV membrane would be less fluid. There was a significant increase to 60% in the amount of cc-siRNA retained in the pellet when the incubation temperature was increased to 22°C. Incubating at 37°C resulted in 66% of the cc-siRNA being pelleted, and at 42°C, 75% of the original quantity of cc-siRNA was retained in the pellet (Figure 2A). In each control condition, only low amounts (3%–9%) of cc-siRNA were retained in the pellet in the absence of EVs.

The incubation time of the co-incubation of EVs with cc-siRNA was then varied while maintaining a constant ratio of 30 cc-siRNA molecules per EV in 100 µL at 37°C. In all samples the majority of siRNA was retained in the pellet (Figure 2B). This was lowest (54%) for a 30 min incubation time but increased to 75% for a 1 hr incubation time. There was no further increase in siRNA retention with increasing incubation time. Similar to the result from Figure 2B, there was negligible signal from the samples without EVs.

Next, EVs were mixed with cc-siRNA at a ratio of 30 cc-siRNA molecules per EV, at 37°C, for 1 hr at varying incubation volumes. For volumes up to 100 µL, a stepwise increase in cc-siRNA retention was detected in the pellet (Figure 2C). For a 10 µL incubation volume, 33% of the cc-siRNA was pelleted; for 20 µL, this increased to 42%; for 50 µL, 57%; and for a 100 µL incubation volume, 74% of the original quantity of cc-siRNA was retained in the pellet. This decreased to 29% with an incubation volume of 500 µL.

Finally, increasing numbers of EVs were co-incubated with a fixed amount of cc-siRNA (resulting in increasing EV:cc-siRNA ratios). A sample without EVs was also included. Incubations were done at room temperature in a 100 µL reaction volume with 30 min incubation time. Following the incubation, EVs were isolated by ultracentrifugation, and the level of cc-siRNA in the pellet was quantified. The highest EV:cc-siRNA ratio tested, 15 cc-siRNA molecules per EV,

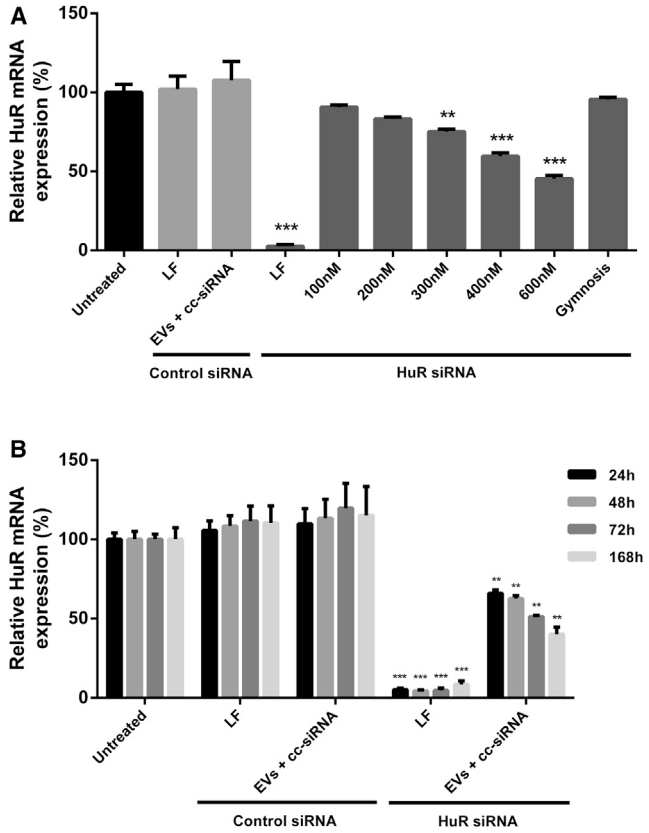

Figure 3. Dose Response and Duration of Silencing in HEK293 Cells Treated with cc-siRNA-Loaded EVs at Optimized Conditions

(A) HEK293 cells were treated with cc-siRNA-loaded Neuro2a EVs at final concentrations of 100, 200, 300, 400, and 600 nM cc-siRNA. EVs were loaded by incubating EVs with cc-siRNA using a ratio of EVs:cc-siRNA of 1:15 at 37°C for 1 hr in 100 μL. *HuR* expression relative to *GAPDH* and *ACTB* was measured 48 hr post-treatment with EVs loaded with a control or *HuR* cc-siRNA or transfection with control siRNA or *HuR* cc-siRNA (600 nM). The effect of gymnosis was evaluated through the inclusion of cells treated with cc-siRNA (600 nM) in the absence of EVs or a transfection reagent. (B) HEK293 cells were treated with cc-siRNA-loaded Neuro2A EVs at 400 nM. EVs were loaded by incubating EVs with cc-siRNA using a ratio of EVs:cc-siRNA of 1:15 at 37°C for 1 hr in 100 μL. *HuR* expression relative to *GAPDH* and *ACTB* was measured 24, 48, 72, and 168 hr post-treatment with EVs mixed with a control or *HuR* cc-siRNA or transfection with control siRNA or *HuR* cc-siRNA (400 nM), or left untreated. Values represent mean + SEM. n = 3. Statistical differences were calculated by one-way ANOVA followed by Tukey's post hoc analysis. Statistical differences indicated are compared with negative control. ***$p < 0.001$, **$p < 0.01$, *$p < 0.05$.

yielded the highest cc-siRNA retention, with 74% of the original quantity of siRNA being retained (Figure 2D). For a ratio of 30 cc-siRNA molecules per EV, the retention was 60% and dropped to 22% when there were 150 molecules of cc-siRNA for every EV, and just 11% when there were 1,500 cc-siRNA molecules per EV.

Based on these results, subsequent experiments were performed using conditions that resulted in the highest siRNA retention percentage, incubating 15 molecules of cc-siRNA per EV at 37°C for 1 hr in 100 μL. Under these conditions, no siRNA retention was observed when EVs were mixed with unconjugated siRNA, demonstrating the critical importance of the cholesterol moiety for the interaction with EVs (Figure S1A). Although more cc-siRNA was retained at 42°C, the risk of EV damage as a result of protein denaturation at elevated temperatures was deemed too high to proceed with this incubation temperature. To investigate whether the association with the cc-siRNA affected EV characteristics, we analyzed the size distribution and EV marker expression after EVs were incubated with cc-siRNA. Compared with untreated EVs, NTA analysis showed a shift in size distribution to slightly larger vesicles following the incubation, with a mode particle size shift of 99 to 109 nm (Figure 1D). The shape of the size distribution curve remained constant and EV marker expression was unchanged (Figures 1C and 1E), suggesting that EV integrity was not affected.

Examining the Functionality of cc-siRNA Delivered by EVs Loaded by Co-incubation

To evaluate whether EVs could functionally deliver cc-siRNA to recipient cells, we added *HuR*-cc-siRNA-loaded EVs to HEK293 cells at increasing cc-siRNA doses. Forty-eight hours following treatment, RNA was extracted from the cells and *HuR* expression levels measured relative to *GAPDH* and *ACTB* (Figure 3A).

We observed a dose-dependent increase in silencing activity of the cc-siRNA-loaded EVs from 11% at 100 nM to 56% silencing at 600 nM (Figure 3A). At 600 nM, no reduction in expression of *HuR* was found for cc-siRNA in the absence of EVs, indicating that cc-siRNA does not enter cells in the absence of EVs or a transfection reagent in a process known as gymnosis.[22] EVs loaded with control siRNA showed no effect. In addition, no reduction in *HuR* expression was observed after addition of an equal number of EVs mixed with unconjugated siRNA (Figure S1B). Significant knockdown was also observed when EVs were added to N2A, SH-SY5Y, or GM04281 cells (Figures S2A–S2C), and when cc-siRNA-loaded, primary dendritic-cell-derived EVs were added to HEK293 or GM04281 cells (Figures S2D and S2E).

We also determined the time dependency of the knockdown effects by adding cc-siRNA-loaded EVs to HEK293 cells at 400 nM and analyzing *HuR* expression after various incubation times. A stepwise increase in silencing efficiency was observed from 36% silencing after 24 hr up to 59% silencing after 168 hr (Figure 3B).

DISCUSSION

One major limitation for translation of EVs to therapeutic use is the lack of an efficient, robust, and scalable method to load them with RNA molecules of interest. This study aimed to evaluate and optimize a method for loading EVs with siRNA via a hydrophobic cholesterol modification to the siRNA. Loading the cc-siRNA via co-incubation with isolated EVs was optimized for the ratio of EVs to cc-siRNA, as well as incubation temperature, volume, and time.

The feasibility of using EVs loaded with hydrophobically modified siRNAs therapeutically was recently shown by Didiot et al.[20] They

also used co-incubation to load EVs with hydrophobically modified siRNA (hsiRNA). Their hsiRNA was modified with a 3′ cholesterol TEG and contained a shorter duplex strand compared with the cc-siRNA used in the present study. Although Didiot et al.[20] reported no change in size following co-incubation of exosome-like vesicles (ELVs) with hsiRNA, they did notice a lower zeta potential (surface charge) of hsiRNA-loaded EVs when mixed with increasing hsiRNA concentrations indicating that their hsiRNA does indeed associate with the vesicle membrane. Despite the absence of a change in vesicle size, their loaded EVs were also capable of functional delivery. They generated a dose-dependent decrease of Huntingtin mRNA and protein expression in mouse primary cortical neurons. On direct brain infusion, the EVs loaded with the hsiRNA resulted in silencing of up to 35% Huntingtin mRNA bilaterally. In the absence of EVs, the hsiRNA and resultant silencing were restricted to the ipsilateral side because of their hydrophobicity.[23]

At the same time, Stremersch et al.[19] demonstrated association of cc-siRNA with ELVs from melanoma and a monocyte/dendritic cell line, and analyzed their siRNA delivery potential. Although isolated slightly differently than the EVs used in the present study (i.e., via differential centrifugation combined with density gradient ultracentrifugation and ultrafiltration), their finding that following co-incubation with cc-siRNA EVs increase in size is in line with the results reported here. The larger vesicle size following co-incubation indicates cc-siRNA is integrating into the membrane so that the cholesterol moiety acts as an anchor for the siRNA. However, they were unable to obtain functional delivery following loading.

A ratio of 1 EV:15 cc-siRNA molecules was found to be optimal, i.e., resulting in the highest siRNA retention percentage, in this study. At higher cc-siRNA densities, the electrostatic interactions between individual cc-siRNA molecules could prevent more efficient loading. Didiot et al.[20] found a maximum of ∼3,000 hsiRNA could be loaded per vesicle but did not test the efficiency of loading at different ratios. Stremersch et al.[19] estimated their ELVs were capable of associating with 73 cc-siRNA molecules. In our hands, the number of siRNA molecules per EV was estimated to be highest at the lowest EV:cc-siRNA ratio tested (i.e., 1:1,500, resulting in ∼165 siRNA molecules per EV), whereas the absolute amount of siRNA loaded in EVs was found to be highest at the highest EV:cc-siRNA ratio tested (i.e., 1:15).

Following the determination of the optimal ratio for association of cc-siRNA with EVs, the temperature, time, and volume of the incubation were varied to establish the optimal conditions for maximum loading. With increasing temperature, the fluidity of the membrane might increase the influence of the lipophilic cholesterol tag on the cc-siRNA and increase association between EVs and cc-siRNA. Temperatures above 42°C were not tested because the EV integrity may be compromised at high temperatures. Therefore, 37°C was selected as the optimal temperature. Interestingly, cholesterol may render the phospholipid bilayer more resilient to heat stress because of its comparatively rigid four-ring structure compared with other lipids in the membrane, if incorporated into the membrane rather than the cc-siRNA being internalized and encapsulated.[24] If this is the case, the integration of cholesterol in the membrane could itself become a limiting factor of association between the EVs and the cc-siRNA by decreasing membrane fluidity.

With regard to the optimal incubation volume, the electrostatic repulsion between the cc-siRNA and the EVs may be high in a small volume, but in a large volume the space between the cc-siRNAs and EVs may be a limiting factor. It is worth noting that with each condition there was low fluorescence in the absence of EVs. This indicates a low contribution of free cc-siRNA to the quantity of cc-siRNA in the pellets of the samples containing EVs.

Having determined the optimal parameters for loading via co-incubation, dose-response and time course experiments were performed to test for functionality of the delivered cc-siRNA. In contrast to the study by Stremersch et al.,[19] where no silencing was observed even though vesicles loaded with cc-siRNA were taken up, here a dose-dependent lasting silencing of the target gene was achieved. Moreover, similar knockdown results were obtained using various other target cells as well as one other EV source cell, suggesting a broad applicability of the loading and gene silencing approach. One possible explanation for this apparent discrepancy is that the nuclease-resistant modifications to the cc-siRNA used in the present study and the study by Didiot et al.[20] may be necessary for the functionality. Other differences could be because of differences in EV source cell and/or isolation technique.

In support of the use of co-incubation as a method for loading EVs, Didiot et al.[20] observed no cytotoxicity, measurable adverse effect on cell viability, or innate immune activation following EV infusion. There was a slight microglial activation at the injection site with EVs, but not by hsiRNA-loaded EVs. This also highlights the potential promise for systemic delivery.

There are several caveats with the use of EV-delivered cc-siRNA here that must be considered. For one, it is not known what effect insertion of cholesterol may have in the EV membrane, because cholesterol could alter the signaling properties of lipid rafts.[25] This effect would need to be tested further.

Second, as seen in this study, large EV quantities are necessary to obtain the observed silencing effects. Thus, a high quantity of EVs would be needed in vivo, and large volumes of EVs could potentially overwhelm physiological clearance systems. It is not known whether the silencing efficiency observed here would be therapeutically relevant because the dose and outcome (silencing as well as pathological and phenotypic measurements) would require monitoring and optimization in vivo. Furthermore, optimization of EV source, siRNA loading efficiency, and siRNA stability and efficacy may help to reduce EV doses. This would also allow comparison between EVs

and state-of-the-art synthetic delivery systems in vivo in terms of siRNA delivery efficiency and safety.

Another potential caveat is that the cc-siRNA may face the extracellular environment. Although cholesterol in a membrane can flip-flop,[26] the hydrophilic siRNA may prevent this. Encapsulated cc-siRNA may not be necessary for silencing in vivo, but for protection from nucleases, intraluminal facing would be preferable, although the modifications of the siRNA used here would increase nuclease stability.

In conclusion, cc-siRNAs associate and co-pellet with EVs and can elicit lasting silencing in vitro in a dose-dependent manner. This straightforward method has the potential to overcome the limitation of poor inefficient loading of EVs with siRNA, which hinders EV research and could help to bring EV-based therapeutics one step closer to clinical use.

MATERIALS AND METHODS

Cell Culture

HEK293 cells (human embryonic kidney cell line), Neuro2A cells (murine neuroblastoma cell line), SH-SY5Y cells (human neuroblastoma cell line), and GM04281 cells (Huntington's disease patient-derived fibroblasts line) were grown and maintained in DMEM (Invitrogen) supplemented with 10% fetal bovine serum (FBS) (Invitrogen) and 1% antibiotic/antimycotic (Life Technologies). For obtaining dendritic cells, all animal procedures were conducted at the Biomedical Sciences Unit, University of Oxford, according to the regulations of the Animals (Scientific Procedures) Act (1986) authorized by the UK Home Office. Bone marrow was flushed from the bone cavity of tibias and femurs of 8- to 10-wk-old C57BL6 mice (The Jackson Laboratory) using a 27-gauge syringe into DMEM. Clumps were dissociated by re-suspension, and samples were centrifuged at 280 × *g* for 10 min. The supernatant was removed and the pellet resuspended in red blood cell lysing buffer (Sigma-Aldrich). Following a 5 min incubation, the suspension was neutralized with DMEM and spun at 280 × *g* for 10 min. Cells were then plated at a concentration of 3×10^6 cells per well in a six-well plate in DMEM, 10% FBS, 1% antibiotics/antimycotic and supplemented with 10 ng/mL murine granulocyte macrophage colony-stimulating factor (GM-CSF) (Sigma-Aldrich) to select for dendritic cells (DCs). All cells were incubated at 37°C in 5% CO_2.

EV Isolation

Cell culture supernatant from Neuro2A or DCs was collected after 48 hr growth in OptiMEM. Conditioned medium was spun at 300 × *g* for 5 min to remove dead and floating cells and 3,000 × *g* for 15 min to remove cell debris. This supernatant was then passed through a 0.22-μm filter and was spun at 120,000 × *g* for 70 min to pellet the EVs using a Beckman Coulter Type 55.2Ti rotor. EVs were resuspended in PBS and underwent a washing step via ultracentrifugation. Pellets were then resuspended in 100 μL PBS by passing the suspension through a 27-gauge needle 10 times. All spins were performed at 4°C.

NTA

NTA was carried out with a NS500 nanoparticle analyzer (NanoSight) equipped with a 405 nm laser to measure the size distribution of particles. A camera level of 15–16 and automatic functions for all post-acquisition settings except for the detection threshold were used. This was fixed at 6. Samples were diluted in PBS between 1:500 and 1:20,000 to achieve a particle count of between 8×10^8 and 13×10^8 particles/mL. The camera focus was adjusted to make the particles appear as sharp dots. Using the script control function, five 30 s videos for each sample were recorded, incorporating a sample advance and a 5 s delay between each recording. During the analysis, the same settings as for the scattering mode were used except for minimum tracking distance, which was set to 5.

Western Blotting

The Invitrogen NuPAGE western blotting system was used as per manufacturer's instructions. Pre-cast gels of 3%–8% tris-acetate from Invitrogen were used. For cells and EVs, 10 μg of protein as measured by Bradford protein assay was used. Antibodies used were ab117600 (Abcam) for Alix, ab30871 (Abcam) for TSG101, and ab22595 (Abcam) for calnexin.

Loading of siRNA by Co-incubation of EVs with cc-siRNA

Varying Ratio of EVs to cc-siRNA

EV number was estimated using NTA, assuming each particle represented one EV. EVs were mixed with cc-siRNA in ratios of 1 EV:15 molecules of cc-siRNA, 1 EV:30 molecules of cc-siRNA, 1 EV:150 molecules of cc-siRNA, 1 EV:300 molecules of cc-siRNA, and 1 EV:1,500 molecules of cc-siRNA. Samples were incubated for 30 min, at room temperature, in 100 μL and washed via ultracentrifugation at 120,000 × *g* for 70 min. The fluorescence of the pellet resuspended in PBS was measured for loading quantification.

Varying Temperature

Ten micrograms of EVs as estimated by the Bradford protein assay kit was incubated with cc-siRNA at a ratio of 1 EV:30 cc-siRNA molecules for 30 min at 4°C, 22°C, 37°C, and 42°C in 100 μL. Samples were then washed via ultracentrifugation at 120,000 × *g* for 70 min. The fluorescence of the pellet resuspended in PBS was measured for loading quantification.

Varying Incubation Time

Ten micrograms of EVs as estimated by the Bradford protein assay kit was incubated with cc-siRNA at a ratio of 1 EV:30 cc-siRNA molecules at 37°C for 30 min, 1 hr, 2 hr, 3 hr, and 5 hr in 100 μL. Samples were then washed via ultracentrifugation at 120,000 × *g* for 70 min. The fluorescence of the pellet resuspended in PBS was measured for loading quantification.

Varying Incubation Volume

Ten micrograms of EVs as estimated by the Bradford protein assay kit was incubated with cc-siRNA for 1 hr at 37°C in 100 μL at a ratio of 1 EV:30 cc-siRNA molecules in volumes of 10, 20, 50, 100, and 500 μL. Samples were then washed via ultracentrifugation at 120,000 × *g* for

70 min. The fluorescence of the pellet resuspended in PBS was measured for loading quantification.

Quantification of Loading Using Fluorescence

Percentage loading was assessed by measuring fluorescence with maximum excitation emission spectrum of 548–570 nm using a Victor3 1420 multilabel fluorescence microplate reader (Perkin Elmer). Fluorescence in each sample was compared with a relative input of Cy-3 siRNA and cc-siRNA alone.

Transfections and EV Treatment

For time course and dose-response evaluations, target cells were seeded at 2×10^5 cells per well in a 24-well plate. After 24 hr, cells were incubated with cc-siRNA-loaded EVs or transfected using Lipofectamine 2000 (Thermo Fisher) according to the manufacturer's instructions. Cells were harvested for RNA extraction following 48 hr for the dose-response study and as stated for the time course evaluation.

RNA Quantification

RNA was extracted from cells using the RNeasy mini kit (QIAGEN) according to manufacturer's instructions. Reverse transcription using the High-Capacity Reverse Transcription Kit (Life Technologies) was used to obtain cDNA from RNA samples, which was used as the template for qPCR using TaqMan Fast Universal Master Mix (2×) (Life Technologies) and the StepOnePlus Real-Time PCR system according to manufacturer's instructions with the TaqMan probes Hs00171309_m1 for *HuR*, Hs01060665_g1 for *ACTB*, and Hs02758991_g1 for *GAPDH* (*GAPDH* and *ACTB* had been determined via GeNorm assays as the optimal housekeeping genes for these studies; Figure S3).

Statistical Analysis

Statistical analyses of the data were performed using Prism 6.0 (GraphPad Software). Data were analyzed by one-way ANOVA followed by Tukey's multiple comparisons post hoc test to assess group statistical significance. Experimental conditions were normalized to a nonspecific negative control unless otherwise indicated. Results are expressed as mean ± SEM, and differences were considered significant at $p \leq 0.05$: $^*p \leq 0.05$, $^{**}p \leq 0.01$, $^{***}p \leq 0.001$.

SUPPLEMENTAL INFORMATION

Supplemental Information includes three figures and can be found with this article online at http://dx.doi.org/10.1016/j.ymthe.2017.03.021.

AUTHOR CONTRIBUTIONS

M.J.A.W. and P.V. conceived the ideas. A.J.O., I.M., O.G.d.J., M.A.V., and P.V. designed, performed, and analyzed experiments. R.M.S. and S.E.A. provided expertise and feedback. A.J.O., M.J.A.W., and P.V. wrote the manuscript. All authors reviewed the manuscript.

CONFLICTS OF INTEREST

S.E.A. and M.J.A.W. declare competing financial interests as founders and shareholders in Evox Therapeutics.

ACKNOWLEDGMENTS

I.M. was supported by an Estonian Research Council Personal Research Grant and European Union FP7/2007-2013 Innovative Medicines Initiative consortium COMPACT (grant 115363). P.V. is supported by a VENI Fellowship from the Netherlands Organisation for Scientific Research (NWO). The authors acknowledge Novartis (David Morrissey and Nicole Meisner-Kober) for providing cc-siRNAs.

REFERENCES

1. Opalinska, J.B., and Gewirtz, A.M. (2002). Nucleic-acid therapeutics: basic principles and recent applications. Nat. Rev. Drug Discov. *1*, 503–514.
2. Vader, P., Mol, E.A., Pasterkamp, G., and Schiffelers, R.M. (2016). Extracellular vesicles for drug delivery. Adv. Drug Deliv. Rev. *106* (Pt A), 148–156.
3. Théry, C., Zitvogel, L., and Amigorena, S. (2002). Exosomes: composition, biogenesis and function. Nat. Rev. Immunol. *2*, 569–579.
4. Simpson, R.J., Jensen, S.S., and Lim, J.W. (2008). Proteomic profiling of exosomes: current perspectives. Proteomics *8*, 4083–4099.
5. Harding, C., Heuser, J., and Stahl, P. (1983). Receptor-mediated endocytosis of transferrin and recycling of the transferrin receptor in rat reticulocytes. J. Cell Biol. *97*, 329–339.
6. Cocucci, E., Racchetti, G., and Meldolesi, J. (2009). Shedding microvesicles: artefacts no more. Trends Cell Biol. *19*, 43–51.
7. Valadi, H., Ekström, K., Bossios, A., Sjöstrand, M., Lee, J.J., and Lötvall, J.O. (2007). Exosome-mediated transfer of mRNAs and microRNAs is a novel mechanism of genetic exchange between cells. Nat. Cell Biol. *9*, 654–659.
8. Alvarez-Erviti, L., Seow, Y., Yin, H., Betts, C., Lakhal, S., and Wood, M.J.A. (2011). Delivery of siRNA to the mouse brain by systemic injection of targeted exosomes. Nat. Biotechnol. *29*, 341–345.
9. Bolukbasi, M.F., Mizrak, A., Ozdener, G.B., Madlener, S., Ströbel, T., Erkan, E.P., Fan, J.B., Breakefield, X.O., and Saydam, O. (2012). miR-1289 and "zipcode"-like sequence enrich mRNAs in microvesicles. Mol. Ther. Nucleic Acids *1*, e10.
10. Koppers-Lalic, D., Hackenberg, M., Bijnsdorp, I.V., van Eijndhoven, M.A.J., Sadek, P., Sie, D., Zini, N., Middeldorp, J.M., Ylstra, B., de Menezes, R.X., et al. (2014). Nontemplated nucleotide additions distinguish the small RNA composition in cells from exosomes. Cell Rep. *8*, 1649–1658.
11. Batagov, A.O., Kuznetsov, V.A., and Kurochkin, I.V. (2011). Identification of nucleotide patterns enriched in secreted RNAs as putative cis-acting elements targeting them to exosome nano-vesicles. BMC Genomics *12* (*Suppl 3*), S18.
12. Akao, Y., Iio, A., Itoh, T., Noguchi, S., Itoh, Y., Ohtsuki, Y., and Naoe, T. (2011). Microvesicle-mediated RNA molecule delivery system using monocytes/macrophages. Mol. Ther. *19*, 395–399.
13. Zhang, Y., Liu, D., Chen, X., Li, J., Li, L., Bian, Z., Sun, F., Lu, J., Yin, Y., Cai, X., et al. (2010). Secreted monocytic miR-150 enhances targeted endothelial cell migration. Mol. Cell *39*, 133–144.
14. Kosaka, N., Iguchi, H., Yoshioka, Y., Takeshita, F., Matsuki, Y., and Ochiya, T. (2010). Secretory mechanisms and intercellular transfer of microRNAs in living cells. J. Biol. Chem. *285*, 17442–17452.
15. Olson, S.D., Kambal, A., Pollock, K., Mitchell, G.M., Stewart, H., Kalomoiris, S., Cary, W., Nacey, C., Pepper, K., and Nolta, J.A. (2012). Examination of mesenchymal stem cell-mediated RNAi transfer to Huntington's disease affected neuronal cells for reduction of huntingtin. Mol. Cell. Neurosci. *49*, 271–281.
16. Wahlgren, J., De L Karlson, T., Brisslert, M., Vaziri Sani, F., Telemo, E., Sunnerhagen, P., and Valadi, H. (2012). Plasma exosomes can deliver exogenous short interfering RNA to monocytes and lymphocytes. Nucleic Acids Res. *40*, e130.
17. Lamichhane, T.N., Raiker, R.S., and Jay, S.M. (2015). Exogenous DNA loading into extracellular vesicles via electroporation is size-dependent and enables limited gene delivery. Mol. Pharm. *12*, 3650–3657.
18. Kooijmans, S.A., Stremersch, S., Braeckmans, K., de Smedt, S.C., Hendrix, A., Wood, M.J., Schiffelers, R.M., Raemdonck, K., and Vader, P. (2013). Electroporation-induced

siRNA precipitation obscures the efficiency of siRNA loading into extracellular vesicles. J. Control. Release *172*, 229–238.

19. Stremersch, S., Vandenbroucke, R.E., Van Wonterghem, E., Hendrix, A., De Smedt, S.C., and Raemdonck, K. (2016). Comparing exosome-like vesicles with liposomes for the functional cellular delivery of small RNAs. J. Control. Release *232*, 51–61.
20. Didiot, M.C., Hall, L.M., Coles, A.H., Haraszti, R.A., Godinho, B.M., Chase, K., Sapp, E., Ly, S., Alterman, J.F., Hassler, M.R., et al. (2016). Exosome-mediated delivery of hydrophobically modified siRNA for Huntingtin mRNA silencing. Mol. Ther. *24*, 1836–1847.
21. Bolognani, F., Gallani, A.I., Sokol, L., Baskin, D.S., and Meisner-Kober, N. (2012). mRNA stability alterations mediated by HuR are necessary to sustain the fast growth of glioma cells. J. Neurooncol. *106*, 531–542.
22. Stein, C.A., Hansen, J.B., Lai, J., Wu, S., Voskresenskiy, A., Høg, A., Worm, J., Hedtjärn, M., Souleimanian, N., Miller, P., et al. (2010). Efficient gene silencing by delivery of locked nucleic acid antisense oligonucleotides, unassisted by transfection reagents. Nucleic Acids Res. *38*, e3.
23. Alterman, J.F., Hall, L.M., Coles, A.H., Hassler, M.R., Didiot, M.C., Chase, K., Abraham, J., Sottosanti, E., Johnson, E., Sapp, E., et al. (2015). Hydrophobically modified siRNAs silence Huntingtin mRNA in primary neurons and mouse brain. Mol. Ther. Nucleic Acids *4*, e266.
24. Papahadjopoulos, D., Nir, S., and Oki, S. (1972). Permeability properties of phospholipid membranes: effect of cholesterol and temperature. Biochim. Biophys. Acta *266*, 561–583.
25. Rosa, P., and Fratangeli, A. (2010). Cholesterol and synaptic vesicle exocytosis. Commun. Integr. Biol. *3*, 352–353.
26. Bennett, W.F., MacCallum, J.L., Hinner, M.J., Marrink, S.J., and Tieleman, D.P. (2009). Molecular view of cholesterol flip-flop and chemical potential in different membrane environments. J. Am. Chem. Soc. *131*, 12714–12720.

YMTHE, Volume *25*

Supplemental Information

Functional Delivery of Lipid-Conjugated siRNA by Extracellular Vesicles

Aisling J. O'Loughlin, Imre Mäger, Olivier G. de Jong, Miguel A. Varela, Raymond M. Schiffelers, Samir El Andaloussi, Matthew J.A. Wood, and Pieter Vader

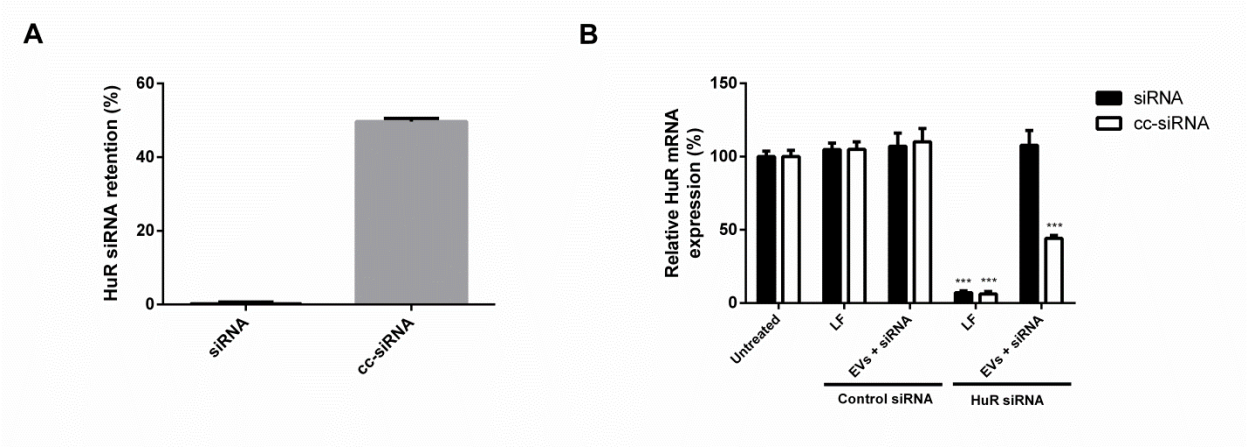

Figure S1. Cholesterol conjugation is critical for successful siRNA loading into EVs and subsequent HuR silencing in HEK cells. A) siRNA retention in pellet following mixing of EVs derived from Neuro2A cells with unconjugated siRNA or cc-siRNA. EVs were mixed with fluorescent siRNA at a ratio of 1:15 at 37 °C for 1 hour in 100 µl PBS. B) HEK293 cells were treated with cc-siRNA loaded Neuro2a EVs at a final concentration of 600 nM cc-siRNA or with an equal number of EVs loaded with unconjugated siRNA. EVs were loaded by incubating EVs with siRNA or cc-siRNA using a ratio of EVs:siRNA of 1:15 at 37 °C for 1 hour in 100 µl PBS. *HuR* expression relative to *GAPDH* and *ACTB* were measured 48 hours post-treatment with EVs loaded with a control or *HuR* cc-siRNA or transfection with control siRNA or *HuR* cc-siRNA. Values represent mean + SEM. n = 3. Statistical differences were calculated by one-way ANOVA followed by Tukey's post hoc analysis. Statistical differences indicated are compared with negative control. ***p<0.001, **p<0.01, *p<0.05.

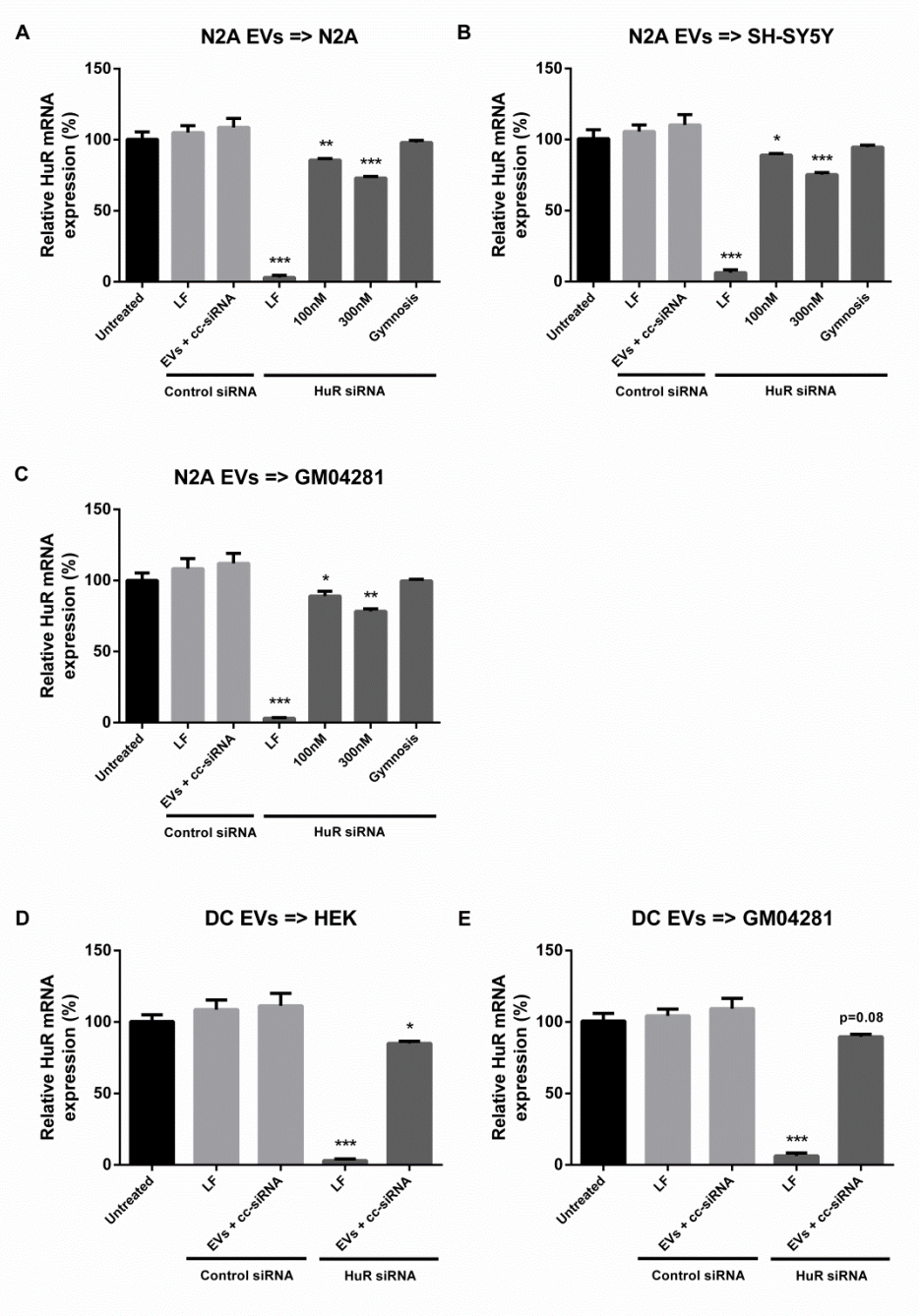

Figure S2. HuR silencing in various cell types treated with cholesterol conjugated siRNA-loaded extracellular vesicles at optimised conditions. A) Neuro2a (N2A) cells, SH-SY5Y cells, GM04281 cells, or HEK293 (HEK) cells were treated with cc-siRNA loaded Neuro2a EVs (A-C) at final concentrations of 100 and 300 nM cc-siRNA or with cc-siRNA loaded dendritic cell (DC) EVs (D,E) at a final concentration of 100 nM cc-siRNA. EVs were loaded by incubating EVs with cc-siRNA using a ratio of EVs:cc-siRNA of 1:15 at 37 °C for 1 hour in 100 µl. *HuR* expression relative to *GAPDH* and *ACTB* were measured 48 hours post-treatment with EVs loaded with a control or *HuR* cc-siRNA or transfection with control siRNA or *HuR* cc-siRNA. The effect of gymnosis was evaluated through the inclusion of cells treated with cc-siRNA in the absence of EVs or a transfection reagent. Values represent mean + SEM. n = 3. Statistical differences were calculated by one-way ANOVA followed by Tukey's post hoc analysis. Statistical differences indicated are compared with negative control. ***p<0.001, **p<0.01, *p<0.05.

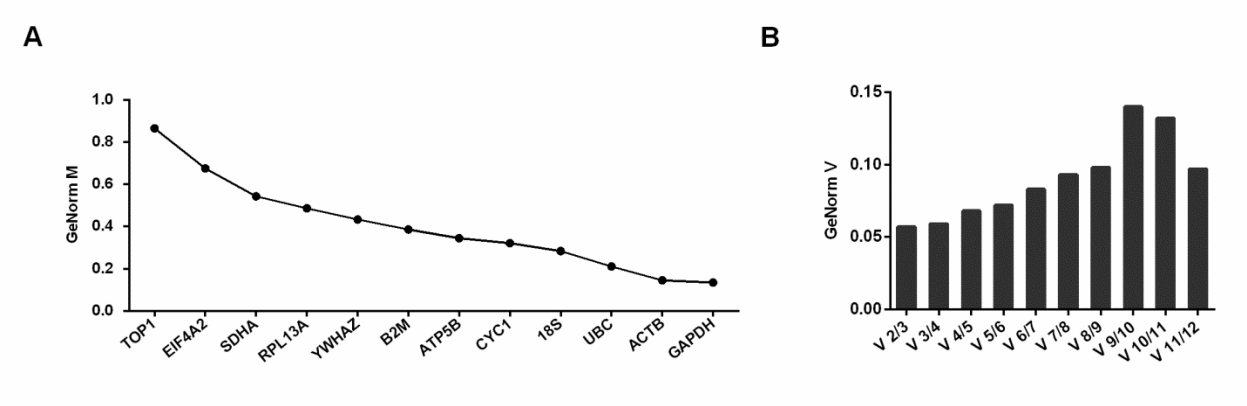

Figure S3: Expression stability (M) analysis and the optimal reference gene number determination with geNorm. The 12 gene geNorm Perfect Probe Plus Mouse and Human Kits (PrimerDesign) were used to identify the most stably expressed and therefore appropriate reference genes for analysis. Using this kit, the expression of 12 candidate reference genes identified from over 30,000 microarray experiments were compared in a representative set of experimental samples. For *in vitro* assessment for HEK293 cells for HTT silencing, samples included untreated cells (n=2), and cells treated with a mid-range dose of each of the therapeutic nucleic acids (n=2). The expression of each of the 12 candidate reference genes was assessed by qPCR using 25 ng of cDNA. **A)** Data was analysed using qbase+ software (Biogazelle) which ranked the candidate reference genes by their gene expression stability (geNorm M). In this study the optimal reference genes, those with highest stability (lowest geNorm M), were GAPDH and ACTB. **B)** Pairwise variation was used to calculate the optimal number of reference genes for normalisation (GeNorm V). All V (n/n+1) values, including V2/3, were below 0.15 in each pool, which indicated that combination of the geometric mean of the two genes was optimal for normalization.